

28476

NAME OF AUTHOR/NOM DE L'AUTEUR

VOS, EDUARD

TITLE OF THESIS/TITRE DE LA THÈSE

THE BEHAVIOR AND THE FRACTURE OF STEEL UNDER CONDITIONS OF EXPLOSIVE LOADING

UNIVERSITY/UNIVERSITÉ

CONCORDIA

DEGREE FOR WHICH THESIS WAS PRESENTED/

GRADE POUR LEQUEL CETTE THÈSE FUT PRÉSENTÉE

M. ENG (MECHANICAL)

YEAR THIS DEGREE CONFERRED/ANNÉE D'OBTENTION DE CE DEGRÉ

1976

NAME OF SUPERVISOR/NOM DU DIRECTEUR DE THÈSE

DR H. J. McQUEEN

Permission is hereby granted to the NATIONAL LIBRARY OF CANADA to microfilm this thesis and to lend or sell copies of the film.

L'autorisation est, par la présente, accordée à la BIBLIOTHÈQUE NATIONALE DU CANADA de microfilmer cette thèse et de prêter ou de vendre des exemplaires du film.

The author reserves other publication rights, and neither the thesis nor extensive extracts from it may be printed or otherwise reproduced without the author's written permission.

L'auteur se réserve les autres droits de publication; ni la thèse ni de longs extraits de celle-ci ne doivent être imprimés ou autrement reproduits sans l'autorisation écrite de l'auteur.

DATED/DATE

APRIL 5 1976

SIGNED/SIGNÉ

PERMANENT ADDRESS/RÉSIDENCE FIXE

15 PRINCE ST.

MONTREAL - Q. 16

H3C 2M7

INFORMATION TO USERS

THIS DISSERTATION HAS BEEN
MICROFILMED EXACTLY AS RECEIVED

This copy was produced from a microfiche copy of the original document. The quality of the copy is heavily dependent upon the quality of the original thesis submitted for microfilming. Every effort has been made to ensure the highest quality of reproduction possible.

PLEASE NOTE: Some pages may have indistinct print. Filmed as received.

Canadian Theses Division
Cataloguing Branch
National Library of Canada
Ottawa, Canada K1A 0N4

AVIS AUX USAGERS

LA THESE A ETE MICROFILMEE
TELLE QUE NOUS L'AVONS RECUE

Cette copie a été faite à partir d'une microfiche du document original. La qualité de la copie dépend grandement de la qualité de la thèse soumise pour le microfilmage. Nous avons tout fait pour assurer une qualité supérieure de reproduction.

NOTA BENE: La qualité d'impression de certaines pages peut laisser à désirer. Microfilmée telle que nous l'avons reçue.

Division des thèses canadiennes
Direction du catalogage
Bibliothèque nationale du Canada
Ottawa, Canada K1A 0N4

THE BEHAVIOR AND THE FRACTURE OF STEEL UNDER
CONDITIONS OF EXPLOSIVE LOADING

by

EDUARD VOS

A MAJOR TECHNICAL REPORT

in

THE DEPARTMENT

of

MECHANICAL ENGINEERING

Presented in partial fulfillment of the require-
ments for the Degree of Master of Engineering at

CONCORDIA UNIVERSITY

MONTREAL - CANADA

March 1976

CONCORDIA UNIVERSITY
FACULTY OF ENGINEERING

Graduate Studies

This is to certify that the Major Technical Report Prepared

By Eduard Vos

Entitled The behavior and the fracture of steel

under conditions of explosive loading

Complies with the regulations of this University and meets the accepted standards with respect to originality and quality.

For the degree of:

Master of Engineering

Signed by the examining committee:

Hugh McQueen
Supervisor

Prof. Hugh McQueen

T.S. Sankar

Prof. T.S. Sankar

R. A. Petkovic

Dr. R.A. Petkovic

M.P. duPlessis

Prof. M.P. duPlessis

Chairman, Dept. of

Approved, for and on behalf of the Dean of Engineering.

J.C. Sign
Assistant Dean, Academic Programmes

Table of Contents

Page

Acknowledgement

1. <u>Abstract</u>	
2. <u>Introduction</u>	
3. <u>Explosives</u>	5
3.1 General Properties	5
3.2 Methods of Loading	7
3.3 Pressure vs. Time Relationships	13
4. <u>Impulsive Waves</u>	16
4.1 General Properties	16
4.2 Reflection and interaction	17
5. <u>Behavior of Iron under High Pressures</u>	20
5.1 Phase Transition & Wave Behavior	20
5.2 The Structure of Iron	23
6. <u>Fracture under Impulsive Loading</u>	30
6.1 Classification	30
6.2 Tensile Fractures	31
6.2-1 Spalling	31
6.2-2 Corner, Cone & Centerline Fractures	47
6.2-3 Radial Fractures	53
6.2-4 Fractures in Pressure Relief Phase	55
6.3 Shear Fractures	62
6.4 Cutting of Metals with Explosives	66
7. <u>Dislocations and Shock Waves</u>	70
8. <u>Conclusion</u>	72
9. <u>Literature List</u>	75

List of Tables and Figures

	Page
Table 1. Some explosives and their properties	5-a
Fig. 1 Schematic representation of explosion	6
Fig. 2 Shock pressure vs. velocity in air	8
Fig. 3 Shock pressure vs. velocity in water	8
Fig. 4 Pressure vs. time for TNT in water	9
Fig. 5 Pressure vs. distance to charge (TNT)	10
Fig. 6 Wave shape vs. distance to charge	11
Fig. 7 Methods of loading specimens	12
Fig. 8 Pressure vs. particle velocity for some metal-explosive systems	13
Fig. 9 Amplitudes incident and reflected waves	17
Fig. 10 Change in wave shape vs. pressure	19
Fig. 11 Hugoniot for various metals	20
Fig. 12 Hugoniot for iron	20
Fig. 13 High pressure phase diagram for iron	21
Fig. 14 Three level pressure wave in iron	22
Fig. 15 Reflection of waves in iron	22
Fig. 16 Shock twins in iron	24
Fig. 17 A twin in δ cc iron	25
Fig. 18 Hardness vs. distance and twin directions	26
Fig. 19 Hardness vs. distance to charge in iron	26
Fig. 20 Shock twins in Ferrite and pearlite	27
Fig. 21 Hardnesses caused by quasi-static loading and by impulsive wave	28
Fig. 22 Metal lattice in compressive wave	29

	Page
Fig. 23 -a Reflection of saw tooth shaped wave	34
-b Reflection of high level wave in iron	35
Fig. 24 Multiple spalling in iron	35
Fig. 25 Cracking and twinning in steel	41
Fig. 26 Spalling stresses in copper & aluminium	41
Fig. 27 "Cavitation" in iron at 300 °C	43
Fig. 28 Schematic formation of corner- and center line fractures	48
Fig. 29 Cratering and fractures in a steel plate	49
Fig. 30 Cone fracture in brass cylinder	50
Fig. 31 Corner fracture in polyethylene	51
Fig. 32 Fractures in internally loaded cylinder	55
Fig. 33 Fractured rod by exterior coating	55
Fig. 34 Bifurcation Crack length (drilling pipe)	55
Fig. 35 Surface texture of drilling pipe fracture	59
Fig. 36 Bifurcation cracks in drilling pipe	62
Fig. 37 Fields of maximum shear stresses	63
Fig. 38 Fractures in externally loaded cylinder	63
Fig. 39 Fractures near explosive in drilling pipe	64
Fig. 40 Structure of drilling pipe	65
Fig. 41 Cutting with a shaped charge	67
Fig. 42 Liner of shaped charge	67
Fig. 43 Hole in steel caused by a shaped charge	68
Fig. 44 Model for super sonic dislocation	71

ACKNOWLEDGEMENT

The author wishes to express his special appreciation to Dr. Hugh J. McQueen who gave inspiration and guidance during his study and for the assistance to bring about this report.

The author also thanks Miss Diane Gaudreau and Mrs Olivia Torres for the typing of the report.

1. ABSTRACT

The purpose of this report is to examine present day knowledge in the field of the behavior and of the fracture of steel under explosive loading. Some fractures observed by the author are discussed.

Explosives and their properties are discussed as well as the type of shock waves that they may cause in metals. The high pressure properties and the micro structure of shock loaded steel are considered. The various fracture phenomena in steel that are caused by explosive loading are examined. Special attention is given to the spalling phenomenon. The fractures in a steel drilling pipe that was exposed to an accidental explosion are examined in some detail. The cutting of metals with shaped explosives is briefly discussed as well as the available theories of dislocation behavior in explosive waves.

Title: The behavior and the fracture of steel under conditions of explosive loading.

Author: Eduard Vos.

2. INTRODUCTION

The rapid loading of metals has been extensively studied as this condition is often found in ordinary engineering structures. In the most common acceptance tests for the impact resistance of steels- the Charpy-V notch or the Izod tests- specimens are broken by a hammer that moves at a velocity of 4.5 m/s (15 ft/s). Pressure waves in steel can travel at the dilatational wave velocity of 5950 m/s (19,500 ft/s) or 1300 times faster than the hammer velocity. This means that the stress that causes fracturing is distributed across the specimen at a much higher rate than the rate of loading. The various points of the cross section of the specimen will be loaded in a gradual and continuous manner until failure takes place. In many industrial or traffic accidents failures are found that involve impact velocities in the order of 30 to 100 m/s (100 to 330 ft/s). The fracture of metals with projectiles involves impact velocities of roughly 300 to 1200 m/s (1000 to 4000 ft/s). The fracture of metals due to chemical explosions involve impact rates in the order of 3000 to 10,000 m/s (9000 to 30,000 ft/s). Meteorite impacts in satellite applications involve impact velocities in the order of 30,000 m/s (100,000 ft/s).

The purpose of this report is to examine the behavior and the fracture of metals, primarily steel,

due to chemical explosions. This type of loading is called impulsive loading. It is in this type of loading that the specimen fails due to a stress wave rather than to a nearly uniform stress condition. An impulsive load is characterized by an almost instantaneous (less than one micro second) increase in load to a high, but finite value followed by a rapid decrease in load. Impulsive shock waves have durations of several micro seconds.

An elastic pressure wave in steel traveling at 5950 m/s takes four micro seconds to travel through one inch of steel. The maximum crack propagation velocity observed for steel is approximately 1800 m/s or 14 micro seconds per inch of fracture length. (1). This speed difference has the result that many separate cracks form prior to the final fracture of the object. The high pressure that occurs in chemical explosions of 3.5 GPa to 40 GPa (5×10^5 to 5.8×10^6 psi) alters the properties of the metal that is exposed to the explosion. Stress waves may travel several times through the metal object before its final shape is reached. It is found that several pressure waves are created from a single pressure wave when the high pressure induces a phase change in the crystal lattice of the metal. Iron is a metal that may undergo such phase change.

The object may not fracture at what is the weakest spot under more conventional forms of loading. The object

will fracture where large-tension or shear stresses are created by the various pressure waves and by the reflections of these waves against free surfaces of the body. The geometrical shape of the exposed metal is important for the fracture behavior because it is the geometry of the body that dictates wave reflections and wave interactions. The shrapnel shape of many metal objects that were subjected to a chemical explosion is the result of the size, the type and the location of the explosive (which determines how and where stress waves will travel) and of the mechanical properties of the object (which determine how well the object can resist the destructive action of the stress waves).

The sudden nature of explosions may often appear to result in chaos. In actual fact the phenomena that take place follow well defined rules and principles and the results of explosions are often as predictable as are more conventional processes.

Explosives are used to alter the shape of metals in the following fields:

- 1) The explosive cutting and fracturing of metals,
- 2) The explosive working of metals,
- 3) The explosive welding of metals,
- 4) The explosive hardening of metals and
- 5) The explosive compaction of metals powders.

Explosives and the type of loading that they may cause will be looked at first. Then the properties of waves traveling through a metal body and the effects of these waves on steel will be discussed. Finally, we shall deal with the various modes of fracture that are caused by impulsive loading. We shall not deal extensively with the various methods of observation nor with the testing apparatus used in the examination of impulsively loaded material.

3. EXPLOSIVES

3.1 General Properties

Explosives are compounds or mixtures of compounds that can be converted in a short period of time to different and more stable compounds, mostly gasses. This reaction is exothermic as approximately 1000 cal per gram of explosive is liberated. The reaction is initiated by heat or by pressure applied to a part of the explosive. From there the reaction front travels in a very short time (at a rate of 1500 to 8700 m/s or 5000 to 28,500 ft/s) through the rest of the explosive mass in the case of "high explosives" and more slowly in the case of "low explosives". Explosive working of metals is generally done with high explosives.

The rate of travel of the reaction front (the detonation rate) is linearly dependent on the density to which the explosive was packed prior to the detonation. The detonation rate is also somewhat dependent on the diameter of the explosive column, on the confinement of the explosive and on the violence of the initiating explosion. For many practical purposes the detonation rate of a particular explosive may be considered as a constant. The table I gives a list of common explosives and their properties (1,2).

Fig. 1 shows schematically how the detonation of an explosive takes place. The front in which the reaction takes place is very thin (0.3 mm for TNT). It moves

Table 1. Some explosives and their Properties

Explosives & Formulas	Energy delivered cal/gram	Density g/cm ³	Detonation rate (D) m/s(ft/s)	Detonation pressure psi	Detonation temperature °C	Length reaction zone mm	Gas produced cm ³ /g
TNT C ₇ H ₅ N ₃ O ₆	782	1.55	7300 (24,000)	2,200,000	3400	0.3	730
Picric Acid C ₆ H ₃ N ₃ O ₇	830	1.69	2470 (24,500)	2,600,000	3500		675
Tetryl C ₇ H ₅ O ₈ N ₅	988	1.65	7620 (25,000)	2,900,000	3900	0.33	760
Nitro Glycerin C ₃ H ₅ N ₃ O ₉	1486	1.6	8540 (28,000)			0.04	
PETN C ₅ H ₈ N ₁₂ O ₄	1385	*	8080 (26,500)				
Lead Azide PbN ₆	400		4890 (16,000)				
Mercury Fulminate C ₂ N ₂ O ₂ Hg			4890 (16,000)				
Composition B 64% RTX 36% TNT	346	1.71	7930 (26,000)	3,400,000			

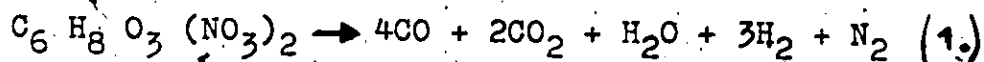
Data from References 1 and 2.

radially outward at a velocity D (See table I).

Fig. 1 Schematic representation of the reaction in an exploding explosive.



An example of the chemical reaction that takes place during detonation is that of cellulose dinitrate:



A total of 980 cm³ of gas at room temperature is created from each gram of explosive.

In an exploding mass there are probably two processes that take place simultaneously:

- 1 - The adiabatic compression from the shock of the detonation heats various points of the explosive mass which then starts to react at many separate points at the same time.
- 2.- The hot reaction gasses ignite remaining un-reacted explosive particles.

There may be localised spots at voids or irregularities in the explosive mass that aid local initiation of the reaction.

An example of what happens after the detonation is the following. The gaseous reaction products of a somewhat confined charge of TNT, packed to a density of

1.5 g/cm³ will reach locally a temperature of 3460°C and a pressure of 20 GPa (3×10^6 psi). The reaction products will flow outward at a velocity of 1750 m/s (5737 ft/s). Pressures in the order of 7 to 20 GPa (3×10^6 psi) can bring profound changes to the structure of a metal. We come back to this subject in chapter 5 when we discuss the pressure dependent phase diagram of iron.

3.2 Methods of Loading

There are essentially three different ways that an impulsive load can be transmitted to the metal object that is to be deformed or to be fractured:

- 1 - A "stand off" charge is detonated in air or in a liquid at a certain distance from the object,
- 2 - A "contact" charge is detonated in direct contact with the object or,
- 3 - The explosive accelerates a projectile or a plate which in turn collides with the target object.

We will discuss these three methods.

3.2.1 Stand off charges

When an explosive is detonated in air or in water, this surrounding medium slows down the expanding gasses while there may be some mixing of the exploding gasses with the medium. The shock wave that is created travels faster than the exploding gasses. Fig's. 2 and 3 show the velocities of the

shock propagation (U) and that of the particle velocities (u) as a function of the peak pressures that occur in air and water respectively. The shock wave travels at 9150 m/s (30,000 ft/s) in air compressed to 0.1 GPa (15,000 psi). The shock wave will finally slow down to the speed of sound in air of 330 m/s (1100 ft/s). The same explosive will create much higher peak pressures in a denser medium such as water.

Fig. 2 Shock wave velocity and particle velocity in air as a function of peak pressure in shock wave.



Fig. 3 Shock wave velocity and particle velocity in water as a function of peak pressure in shock wave. For relatively low intensity shocks.



The explosion of a 3.7 kg (8 lb) TNT charge at 7.5 cm distance below the water surface will create a peak pressure of 2 GPa (300,000 psi) versus 0.1 GPa (15,000 psi) in air. (2) The decay of pressures for water is given by the formula 2.

$$P = P_0 \times r^{-1.13} \quad (2.)$$

with a certain minimum value for r and

in which P is the peak pressure at a distance r from the explosive. The initial peak pressure is P_0 .

Fig. 4 gives pressure versus time curves for a TNT charge detonated in water. As shown in fig. 3 the initial shock wave velocity in water is up to 4600 m/s (15,000 ft/s). The wave gradually slows down - as a function of the peak pressures in the shock wave - to 1500 m/s (5000 ft/s) which is the speed of sound in water.

Fig. 4 Pressure-time curves for TNT charges exploded in water. Distance from charge 1 ft.




Fig 5b gives, as an example, the pressure versus the distance from the charge curves for the TNT charge that is shown in fig. 5a. This charge is 7.5 m long and it weighs 22 kg. The charge is detonated in water. At 18m from the charge the peak pressures are still from 1.2 to 6.9 MPa (175 to 1000 psi). The pressure depends on where it is measured in relation to the shape of the explosive.

Fig. 5a & 5b schematic shock wave (5a) and actual measurements of peak shock pressure (5b) of a 50 lb, 25 ft long TNT charge in water. Detonation at 0 (near end).



The initial pressure is related to the square root of the explosive mass. The positive impulse, the pulse duration and the energy density also depend on the square root of the explosive mass. The impulse (I) of a stress wave is defined as

$$I = \int P dt \quad (3.)$$

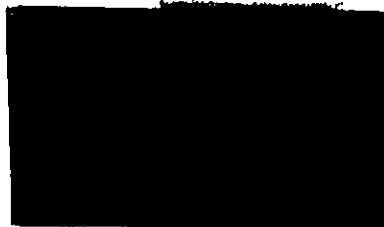
with a certain maximum limit for the time (t). The energy density is defined as the amount of energy that passes a square unit of surface, the surface being perpendicular to the direction of the wave propagation. When the explosive has reacted completely a negative pressure or rarefaction phase develops.

Fig. 6 shows the change in the shape of the impulse wave as a function of the distance to the explosive.

3.2.2 The contact charge

The contact charge may create very high intensity shock waves as there is not the intermediate medium such as air or water that acts somewhat as a buffer. The pressure wave has approximately the shape of t_1 in fig. 6. A shock wave not in contact with the object may have more the shape of t_3 to t_6 of the same figure.

Fig. 6 Overpressure in shock as a function of distance from source at several subsequent times $t_1 \rightarrow t_6$



A contact charge may be placed on the surface of the object, fig. 7, it may be wrapped around the object or it may fill a cavity in the object. It is especially in the last case with the detonation in a confined space that exceedingly high impulses are found. The pressure levels may be approximated by using the general gas law. If an explosive such as cellulose dinitrate has an original density of 1 g/cm^3 and if the reaction takes place at a temperature of 4000°C the static pressure reaches 1.4 GPa (200,000 psi) (Table I). The actual peak pressure obtained is approximately one order of magnitude larger due to the

propagation of a pressure front: the action does not take place at the same time in the entire space available but a reaction front creates a forward particle velocity and a peak pressure.

Fig. 7 Assemblies for subjecting specimens to a plane wave shock. on top two explosives. In center specimen in a specimen plate; a back up plate absorbs the passing wave. The water and the Styro-foam secure undamaged recovery of the specimens.



3.2.3 Impacts

The explosive can be used to accelerate a plate or an other object. The impact of this object creates high-level sharp-fronted waves in the target object. (Fig.7). In the case of an impact of an object as well as with an explosive pressure wave the surface of the metal depresses at a velocity u while the pressure wave travels at a velocity U into the metal. The surface or particle velocity (u) is related to the pressure wave velocity (U), the pressure (P) and the material density (ρ) as follows:

$$u = \frac{P}{U \cdot \rho} \quad (4.)$$

Fig. 8 represents this relationship for various metals. For example the surface of iron in contact with a TNT charge will depress at a velocity 900 m/s (3000 ft/s) and the pressure will be 31 GPa (4,500,000 psi) at the surface. Maximum pressures are reached when the shock wave hits the metal surface head on, however, the angle between the propagation and the surface may decline to about 60° before the peak pressure at the surface is reduced appreciably. Further decrease of the angle will then cause a rapid decrease in peak pressure at the surface.

Fig. 8. Pressure-particle data for several metal-explosive interactions.



3.3 The pressure versus time relationship

An interesting phenomenon in explosive loading, especially in contact operations, is the fact that the times during which peak pressures are maintained are not equal at all points of the surface exposed to the explosion. A great deal depends on the shape of the explosive and on the direction of the impulsive wave. We consider the following cases:

The time during which the pressure is maintained increases linearly with an increasing explosive thickness. The peak pressures maybe sustained for 2 micro seconds and for 4 micro seconds for 12 and 25 mm thick explosives respectively. The peak pressures at the surface do not change directly with thickness, they depend on the square root of the mass of the explosive used. The energy of an explosive pulse is given in terms of the pressure multiplied by the time that the pressure is sustained (see the section 3.2.1). The pressure at the center of a cylindrical charge place on the metal surface will be sustained for a longer time than at the edge of the cylinder. Taking as an approximation that the pressure release wave of the explosion moves at two thirds of the detonation rate, the peak pressure below the center of a one inch diameter explosive maybe maintained for 2 or 3 micro seconds, while at the edge of the charge this is less than one micro second. (1).

In both cases above, the charge was confined on only one side. An explosive placed in a cavity in the metal will create pressures that are sustained for a longer period of time than in the cases detailed. Near the detonator the pressure is felt earlier. Near the bottom of the cavity, i.e. away from the detonator, the pressure is felt last, but it is sustained longest. Confinement retards the pressure relief. The relief wave has to

travel a greater distance to allow a pressure drop at the bottom of the cavity. The peak pressure may be maintained for 3.5 and 7 micro seconds at the bottom of 50 and 100 mm deep explosive filled cavities respectively.

4. IMPULSIVE WAVES

4.1 General

There are three types of impulsive waves: 1) longitudinal or dilatational waves, 2) transverse or shear waves and 3) surface or Rayleigh waves. Only the first two types are generally important in the explosive loading of metals. The longitudinal wave moves fastest at a speed (C_1), which is related to the bulk modulus (K) the density (ρ) and the poissons ratio (ν) as follows: (1)

$$C_1 = \sqrt{\frac{3K(1-\nu)}{\rho(1+\nu)}} \quad (5.)$$

At a moderate pressure steel has a K of 166 GPa, ρ equals 7,800 kg/m³ and ν equals 0.28. The resulting C_1 is 5950 m/s (19,500 ft/s). (1).

The particle velocity (V_p) causing the wave propagation is related to the wave velocity C_1 as follows:

$$V_p = \int_0^{\epsilon} C_1 d\epsilon = \frac{1}{\rho} \int_0^{\epsilon} \frac{dG}{C_1} \quad (6.)$$

These equations allow the calculation of stresses and strains (ϵ) in metal if C_1 and V_p are known. The direction of V_p is in the same sense for a longitudinal compression wave and opposite for a longitudinal tension wave. In a shear or transverse wave the particle velocity is perpendicular to the wave direction. The velocity of a shear wave (C_2) is related to the shear modulus (G) as follows:

$$C_2 = \sqrt{\frac{G}{\rho}} \quad (7.)$$

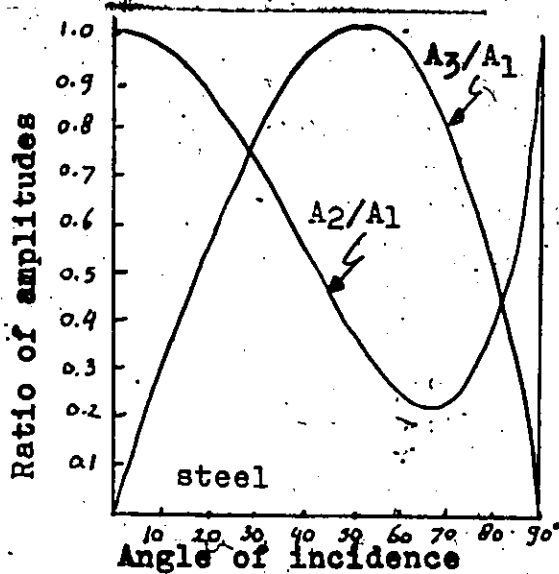
For steel at moderate pressures G equals 79 GPa and the resulting $C_2 = 3200$ m/s (10,500 ft/s).--(1,3,4).

4.2 Reflection and interaction of waves

Without going into a detailed treatment of pressure waves we give the following data. For detail we refer to ref's. 2,5, and 6. A compression pulse will reflect from a free surface or from an interruption in the material such as a different phase, a crack, or an interface with a different material. It will reflect as a tension wave under the same angle as the angle of incidence. It will reflect as a pure tension wave if the angle of incidence is ninety degrees. With an oblique angle of incidence, the tension wave will be accompanied by a polarised shear wave. The angle of reflection of the shear wave is different from that of the tension wave. The energy of the original compression wave is divided between the two types of reflecting waves depending on the angle of incidence. This is shown in fig. 9

Figure 9. Amplitudes of reflected shear and dilatational waves.

- A_1 -incident wave
- A_2 -reflected dilatational wave
- A_3 -Reflected shear wave.



It is the tension component of the reflected wave that may cause fracture when it exceeds the cohesive forces of the metal. This may cause the scabbing or spalling phenomenon that is found at the free boundary that is opposite to the boundary where the compression wave entered the metal. We discuss this scabbing phenomenon further in section 6.2.1. In the corners of the metal body two compression waves that are reflected as tension waves may interfere to reach a value that can cause what is called a corner fracture. The reflected tension and shear waves will reflect again when they reach other surfaces of the metal body. The tension wave will reverse again to become a compression wave, while the shear waves remain as shear waves. After several of such reflections a very complicated stress wave condition exists in the metal body.

If the stress level within the metal becomes such that it is one or two orders of magnitude larger than the static shear stress, the metal assumes certain properties similar to that of a fluid in the sense that it may flow under the influence of shear stresses. In this case a hydrodynamic treatment for the stress waves behavior is used by many researchers (1,7,8). Shear waves do not propagate in liquids. The same is true for metals if the level of the shear wave surpasses that of the shear stress of the metal. The longitudinal hydrodynamic wave

propagates at a velocity (C_1) that equals : (7)

$$C_1 = \sqrt{\frac{K}{\rho}} \quad (8.)$$

in which ρ is the density at the particular pressure and K is the bulk modulus. This is the general case for any metal. Metals become much more difficult to compress after a certain amount of compression; K increases with compression in the following general fashion: (9)

$$K = a p + b p^2 \quad (9.)$$

in which a and b are constants and p is the pressure.

A low level elastic dilatational pulse has a decreasing peak pressure when it propagates (fig. 6). At the same time the wave front becomes steeper. This is because the wave speed at the center of the wave is higher than that at the start of the wave as it propagates in a medium with a larger bulk modulus.

Over a certain pressure range iron is an exception. We come back to this later. Fig. 10 shows how the center of the compressive wave front steepens. The opposite effect is found in a tension wave where the stress wave spreads out. The time of the pressure rises in the steep front is approximately 10^{-7} seconds. The atoms in the metal lattice vibrate with a period of 10^{-14} seconds.

Fig. 10 Schematic representation of shock formation

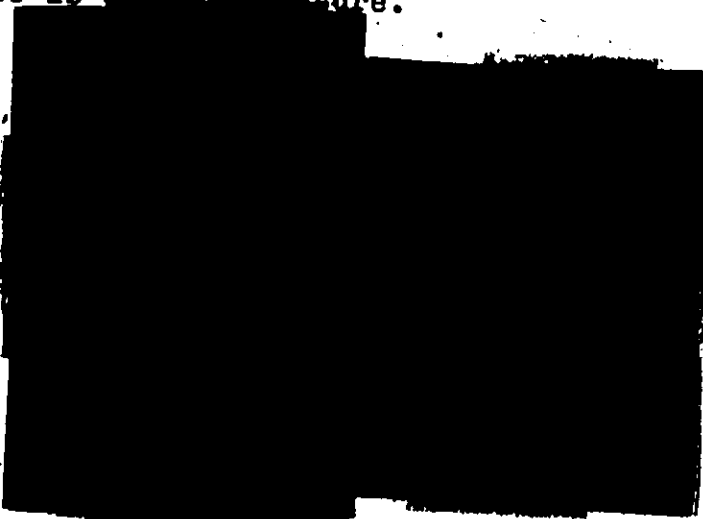


5. THE BEHAVIOR OF IRON UNDER HIGH PRESSURE

5.1 Phase transition and wave behavior

Iron, bismuth and antimony are the only metals known to date that undergo phase transitions when compressed. These three metals have crystal structures that are not most densely packed. It may be logically expected that such structures (bcc or rhombohedral in these cases) can be forced into more densely packed structure (fcc or hcp) by large enough compression. However columbium which is bcc, can be compressed to pressures up to 58 GPa (8,500,000 psi) without a phase transformation. A pressure versus volume curve is also called a Hugoniot curve. Fig's. 11 and 12 gives the Hugoniot for iron. There is a phase change at 13 GPa (1,900,000 psi or 130 k bar) when the iron has been compressed to 93% of its original volume. See figure 12. Then suddenly without substantially raising the pressure the volume will decrease by another 2% when a different phase forms. Researchers up to 1961 (1,10) referred to this phase as a γ phase which is fcc. It was then found that the phase is a δ phase structure.

Figure 11 & 12
Hugoniot curves for
iron and other
common metals
(10 kbar equals 1 GPa)



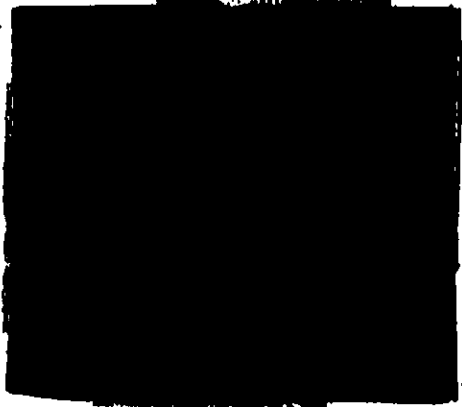


Figure 13 - The high pressure phase diagram for iron.

The formation of this phase (ϵ) has a profound effect on the compression wave from an explosive charge as the wave velocity depends on the slope of the Hugoniot curve. The steeper this Hugoniot curve, the faster a wave will travel. It has been found (5) that between pressures of 13 and 34 GPa (1,900,000 and 5,000,000 psi) the pressure wave will travel slower than below or above these values. As a result of this phase transition a high level shock wave in iron has been found to split up into three distinct different waves:(7,11)

- 1) A low level elastic (precursor) wave of 1 GPa (150,000 psi)
- 2) A plastic I wave of 13 GPa (1,900,000 psi) which is followed by
- 3) A plastic II wave with approximately the original peak pressure of the explosion.

The three waves are shown schematically in figures 14 and 15. The distance between the waves is determined by

the level of the peak pressure and by the duration of the applied pressure. It is the plastic II wave that is responsible for the phase transformation. The effects of this wave are discussed in chapter 6.2. Some researchers only mention the final two waves (12) presumably as the elastic precursor wave found by others (7,11) is small, 8% of the plastic wave I, and thus less significant.

Fig. 14 Idealized pressure profile of compressive shock wave in iron.

D₁₀ is the precursor Wave
D₂₁ is the Plastic I wave
D₃₂ is the Plastic II wave



Fig. 15 Pressure profiles of compressive wave with three discrete shocks being reflected from a free surface. Rarefactions also shown as discontinuities, though actually these would become ogives.



We note that research in this high pressure area is of use in astrophysics and seismology, while in metallurgy the stress wave behavior can be used for the study of phase transformations. Interesting work was done by Pipkorn (9) using a static pressure cell and the iron isotope Fe^{57} . It is mentioned that α iron is still found between 13 GPa and 30 GPa (1,9 and 4,3 million psi) as the $\alpha \rightarrow \epsilon$ transformation can be rather sluggish under static loading. This may be an additional factor why the parameter of time in explosive loading is important. The ζ phase iron is antiferro magnetic, while χ phase iron is para magnetic (9,10).

5.2 The structure of iron

The structure of iron exposed to the $\alpha \rightleftharpoons \epsilon$ phase transformation is quite different from adjacent untransformed iron. Microscopically, such a region shows up as an area that etches darker than the adjacent iron. The volume of the space that underwent the phase transition is approximately 4 to 5 times greater than the volume of the cone shaped crater that is left by a contact detonation. The transformed area lies below the crater and its cross section has a semi-elliptical shape (13). Close to the crater surface there are severely deformed ferrite grains. Slightly further down but still in the dark etching zone, there is a fine widmanstätten structure in the ferrite grains rather like the structure found in ferrous meteorites.

A Widmanstätten structure is a structure characterized by a geometrical pattern resulting from the formation of a new phase (ϵ) along certain crystallographic planes in the parent solid solution. Pearlite retains more or less its original shape and appearance. This dark etching region will usually not fracture during the initial wave passage as the large pressures tend to push the atoms together rather than to separate them (14,15,16). Only shear fractures are possible under such high compressive stresses in conditions of plane stress.



Fig. 16 Photomicrographs showing microstructure of favorably oriented ferrite grains. (a) six twin directions, (b) seven twin directions.

Below the dark etching region, i.e. further away from the explosive, we find a structure with "shock twins" or "Neumann bands". Near to the dark etching region we find ferrite that has twinned in 5 (17), 6 or 7 (18) different directions. As we move away from the dark etching region, the number of twin directions decreases. Fig. 16 shows such shock twins. Fig. 17 shows a twin in α iron. Fig. 18 and 19 show that the hardness of the steel decreases in a step form and that the amount of twin directions would correspond with the hardness plateaus. These steps are also reported by different researchers (1). In work on single crystals, only faint hardness plateaus and a more gradual decrease in hardness as well as in the number of twins was found (17); The number of twinning directions was uniform over the entire range away from the source of the explosion. The general direction of markings in the dark etching zone is the same as in the underlying twinned region (17). In a ferrite-pearlite structure, the twins in the ferrite may propagate in the same direction in adjacent pearlite. This phenomenon is described in references 12 and 17. (See fig. 20) The shock twinned region may be found from one to seven inches away from the explosive. Nowhere in the twinned region is there evidence of slip or grain boundary distortion. Twins that formed at pressures above 31 GPa (4,500,000 psi) are simpler and thinner in appearance. All twins lie on (211) planes (17,19). The

same is true for Neumann bands that are formed by conventional deformation of steel at low temperatures.

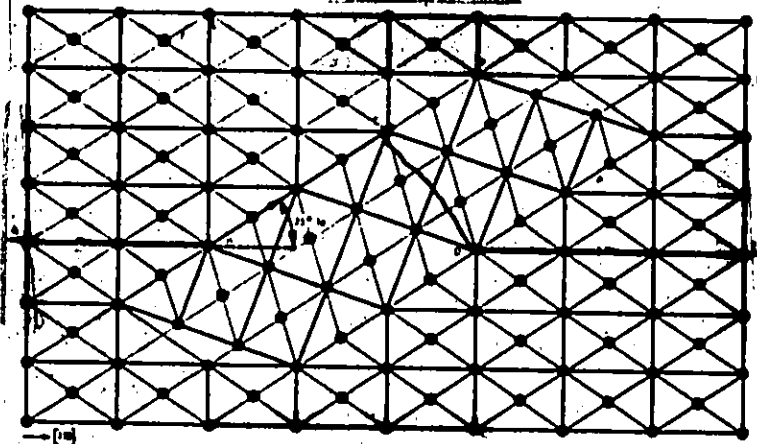


Fig. 17 Cut along (110) plane through a coherent twin in a bcc lattice.



Fig. 18 Typical hardness curve and twin directions plotted from data taken along a radius of a circular cross section of the target.

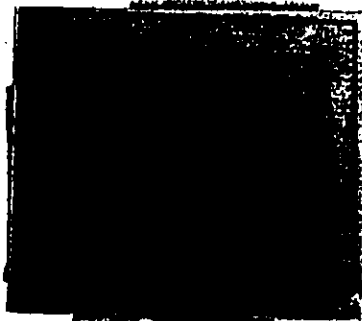
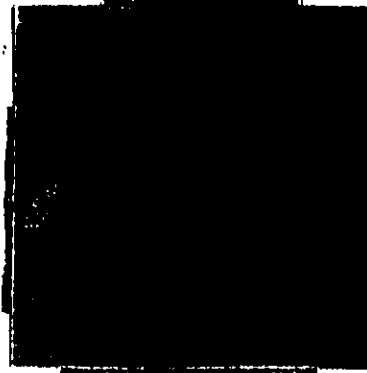


Fig. 19 Hardness curve plotted from data taken across a Section of a Thick-walled Low Carbon Steel Cylinder with explosive (9 inches o.d. by 1 inch i.d. by 6 inches cylinder). Explosive inside Cylinder.

Fig. 20 Twins in ferrite propagate into pearlite. 100X

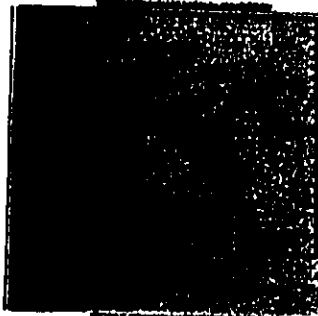


The hardness profile given in figures 18 and 19 is not easily explained. In conventional work hardening there is a certain change of shape at ambient or at low temperatures that creates slip and dislocation pile-ups to explain the hardening effect (27,43). In the case of explosive loading there is no or very little over-all deformation and no microscopically visible grain distortion in the twinned region. Iron subjected to 41 GPa (6 million psi) pressure will be as hard as 95% cold reduced iron without a noticeable grain distortion. This is shown in fig. 21 where the hardnesses of quasi-statically and of dynamically produced similar depression are compared.

Possible explanations for the hardness increase are:

- 1) The twins themselves,
- 2) A distorted lattice as is indicated by X-ray measurements of regions that were subjected to shock waves large enough to cause plastic deformation,
- 3) The presence of point defects in the lattice left by fast moving dislocations. (20)

Fig. 21 Comparison of hardness profiles below an impulsively and a statically formed depression in low carbon steel



There is little evidence to date to support the latter theory; it is possible that the bulk of the dislocations are annihilated at the increased temperature associated with the shock wave. (21). Figures 22 a and b give two models for the metal lattice as it may become during the passage of the shock wave. In the case of the plastic wave in Fig. 22b, one dislocation in 15 rows of atoms is necessary to explain a 20% volume decrease. (22). There is no substantial difference in the hardness of a grain that is twinned and one that shows no twins in the same hardness region of the specimen. As such twins would not explain alone the work hardening of impulsively loaded metal (22). The other proposed explanation for the hardening effect is the presence of point defects left behind by the dislocations in the moving shock front. To date there is insufficient understanding of the atomic processes surrounding the high level plastic pressure waves in metals, including iron. It is not known with certainty in which stage of the impulsive loading shock twins form in iron. It is possible that twins form during the passage of any of the three pressure waves

and that further twinning or "un-twinning" of previously formed twins takes place when the reflected waves travel back through the material. The sequence of the twinning and hardening is important for the fracture of the metal.

Fig. 22 Possible interfaces between normal and compressed lattices. (a) Uniaxial elastic compression; (b) Hydrostatic compression.



6. FRACTURE CAUSED BY IMPULSIVE LOADING

6.1 Classification

6.1.1 Tensile fractures

Tensile forces may result from reflected compression waves. In this case spalling or scabbing occurs at a certain distance from the reflecting face. Corner fractures or center line fractures are a result of the interaction of several reflected tensile waves. In some instances we find micro-cracks that run within one grain or small transgranular cracks when the time available for the formation of such cracks increases. We may find large cracks when the object separates in several pieces during the pressure relief phase of the explosion. The times for the formation of these cracks is larger than for the transgranular cracks.

These large cracks may travel at speeds up to 1,800 m/s (6,000 ft/s). It is then that the crack front may form bifurcation cracks and may follow a wavy path. The tensile fractures are mostly of a brittle or cleavage nature because of the triaxial nature of many such loading conditions and furthermore because the wave propagation takes place at approximately the dilatational wave velocity of 5,950 m/s (ft/s). The dislocations that would cause slip and deformations can only travel approximately half as fast at the shear wave velocity.

6.1.2 Shear fractures

Shear fractures are commonly found in metals that are fractured by an explosion. They are caused by shear components of tension or compression stresses acting upon the metal. Compressional stresses tend to suppress the formation of tensile fractures (the Bridgeman effect). Shear fractures are ductile in nature.

6.1.3 Cutting fractures

The fractures associated with the cutting of metal with the aid of shaped or metal lined charges are not real fractures in the conventional sense of the word: they are rather a cutting by the aimed impact of explosion products or of products accelerated by an explosion. In the latter case a layer of the accelerated material is found fused to the material of the target object.

6.2 Tensile fractures

6.2.1 Spalling

6.2.1.1 General data on spalling - This type of fracture is also called Scabbing or Hopkinson - fracture. Spalling is the same phenomenon that makes the last of a row of billiard balls fly away when the first of the row is hit. In the case of the spalling of metals, a certain critical stress has to be overcome to separate a layer of metal on the side opposite to the application of the

impact. This critical stress is stated to be 1.1 GPa (160,000 psi) for 1020 steel (1). The critical stress varies with the following parameters:

- 1) The shape and the amplitude of the stress wave,
- 2) Material properties such as the dynamic stress-strain curve, the effective surface energy of the material, the composition, the grain structure and the geometry of the piece.

There are presently two theories that deal quantitatively with spalling: one theory takes the gradient of the tension wave front as the critical parameter, the other takes the impulse of the tension wave as parameter. The impulse being defined as the product of the pressure and the time.

Fig's 23 a and b give two possibilities for the pressure wave reflection in steel. The elastic precursor wave (see P.21) is not shown. It has not been shown if or how this wave is involved in the fracture of steel. In case of a single wave front when the peak pressure is below 13 GPa (1.9 million psi) the reflected wave slowly increases from a zero value when the magnitude of the reflected wave is completely compensated by the incoming compression wave. (Fig. 23a). When the reflected wave travels further back into the metal it is compensated by a compressive wave of decreasing size. The peak pressure of the final resulting tension wave

is equal to the peak pressure of the original compressive wave multiplied by a factor between 0 and 1. The factor depends on how much energy is absorbed by the shear wave created in a reflection under an oblique angle of incidence. Fig. 9 shows the relationships between the angle of incidence and the level of the reflected tension and shear waves. It is the decrease in the tension wave as a result of the formation of the shear wave - that limits the surface of the spalled area.

When the peak pressure is enough to allow the formation of ϵ phase iron the net stress during the reflection of the plastic I wave is small, but reflection of the plastic II wave will cause a very steep shock front (see fig. 23b). This is further described when the smooth faced spall is discussed. If the level of tension stress during an initial phase of the wave reflection is large enough to cause a spall, this spall traps the part of the wave that is in the spall. The remainder of the arriving compressive wave will find a new free surface from which it will reflect. It is in this manner that multiple scabs or spalls are formed provided that the initial pressure wave is of sufficient magnitude. (Fig. 23a) The critical fracture stress level for low carbon steel is in the order of 1.16 GPa (160,000 psi) versus 13 GPa (1,900,000 psi) for the

phase change level. A saw tooth shaped pressure wave of the 1,900,000 psi level could theoretically cause 11 different spalls ($1,900,000:160,000 = 11.8$, but partial spalls do not occur). A pressure wave without a gradually decreasing pressure trail could theoretically be trapped in the metal of the first spall before it had the time to travel back into the rest of the metal. Multiple spalling has been found for steel wherein six different spalls could be identified. Fig. 24) The first spall (i.e. the spall furthest away from the explosive) is the largest in surface area. From this spall going toward the source of the explosion the spalls become generally smaller in surface. The tension waves causing the subsequent fractures has been weakened in the reflection against an irregular - rough and grainy-fracture face. This creates a relatively large amount of shear waves to the expense of the tension wave which is the wave that causes spalling. A rough fracture face also creates a less steep wave front.

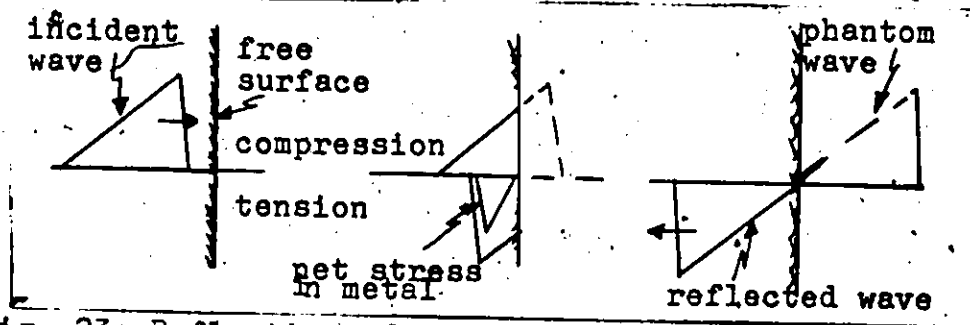


Fig. 23a. Reflection of simple compression wave.

Fig. 23b Schematic
wave reflection for
creation of smooth
spall

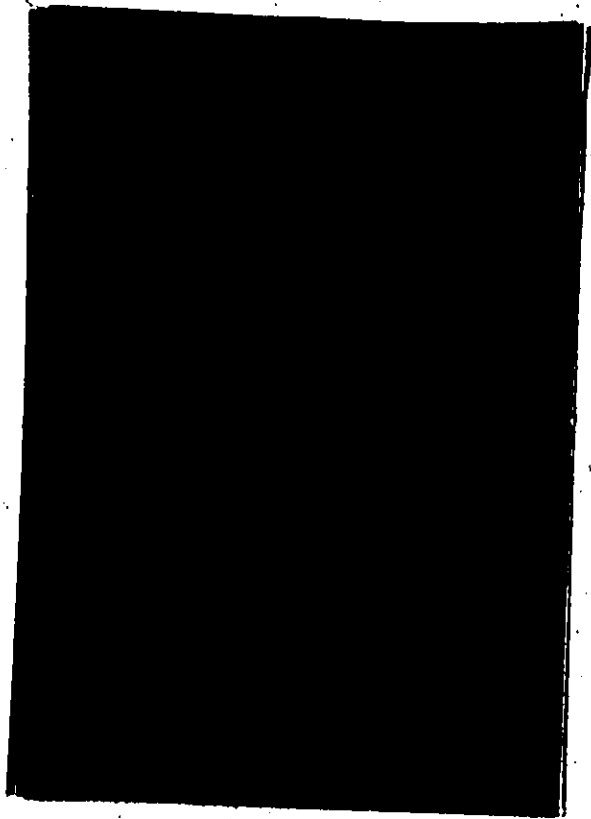


Fig. 24 Multiple
spalling in mild
steel plate (6 inches
dia. x 3 inches thick)



Only the first spall that forms by a wave that has passed through iron may be smooth in appearance; other spalls are rough in appearance. This is discussed in the next section.

The location and the surface area of the spalls can be used to obtain a measure of the size and of the shape of the pressure wave that caused them. The principle of the billiard ball experiment is also used to measure the size and the shape of the pressure wave: At the back of the explosively loaded body one places "billiard balls" or "spalls" of various sizes. These objects are usually finely ground small metal plates of the same composition as the target object. The velocity and the mass of these small plates after an explosive wave separated them from the target object give a measure of the size and of the shape of the explosive wave (1,30).

It is the forward movement of material under the influence of a compressive wave or under the influence of an impact with a foreign body that causes a certain pressure rise in the material. The velocity of the movement of the material maybe called the particle velocity (V_p) or the impact velocity (V_i). The impact velocity that may result in a stress that is large enough to cause spalling is called the critical impact velocity (V_{ic}). For low carbon steel the critical impact velocity is 26 m/s (84 ft/s) (1,2,3) the peak pressure of the wave P as a result of a certain material velocity (V) is given by the formula (4)

$$P = \rho \cdot C_1 \cdot V \quad (10)$$

in which ρ is the material density and C_1 is the dilatational wave velocity. The critical stress for spalling of low carbon steel is 1.1 GPa (160,000 psi).

The effective length of the pressure wave is 37 mm (1-1/2 in.) for waves at the 7 GPa (1,000,000 psi) level created by a contact charge on the surface (23).

The duration of the pressure wave depends, as already discussed, on the size and the magnitude of the charge and on its confinement. The thickness of the spall must be less than half of the length of the pressure wave.

6.2.1.2 The appearance of the spall surface and the mode of fracture.

For stress levels above 13 GPa (1,900,000 psi) with the wave passing through iron in the ϵ phase, a spall may have a smooth surface, while below this level the spalls have a rough surface.

(A) ROUGH FACED SPALLS

The rough faced spalling phenomenon was studied by Banks (24) and by Skidmore (8). The fracture face is of a brittle cleavage nature. The cleavage facets lie on the (100) planes of the lattice. River patterns on the cleavage facets show that the fracture propagated from different directions in adjacent grains. This means that fracture originated simultaneously in many different points. The various cleavage planes may join

by small areas of ductile shear. The presence of shear has been verified by the observation of laterally displaced twins across micro-cracks that were adjacent to the main spalling plane.

The part of the stress wave that causes these fractures has a width of approximately 0.1 mm. This means that the layer subjected to the tensile stress is only one or several grains thick. This stress and fracture condition offers an interesting opportunity to study the crack nucleation process in metals: The fractures lie along the weakest path on a microscopic scale and not along the weakest path on a macroscopic scale. Banks found that the cleavage cracks started in the interface between iron and cementite platelets or cementite films. Another possible mechanism for nucleation of cracks is the bending and cracking of thin cementite layers in the grain boundaries when the ferrite matrix twins. In this case the cracks would start in the cementite itself. Both theories are suggested as the likely crack nucleation processes at low temperatures (-196°C). Transmission electron micrographs of fractures in low carbon steel at low temperatures (25) show that crack and twinning structures are very similar to those taken of spalls with a rough surface appearance (24,25). In neither case were twins found to be the sites of crack nucleation although

many of the twins existed prior to the cracking. Micrograph 25a shows a crack arrest by a twin (25). In some cases (27) twin intersections are found to be crack origins in conventional loading of metals. This has not been found in spalling fractures. I suggest the following explanation for this. Fig. 25 shows that most twins existed prior to the cracks. This means that the twins formed to alleviate the initial compressive waves. The stresses at the twin intersections caused by the compressive waves would thus be compensated by the reflected tensile waves which tend to "un-twin" the existing twins. Work hardening at the twin intersection in the compressive phase creates an unfavorable condition for subsequent tensile fractures. It is possible that the crack formation process at low temperatures at low strain rates is the same as that at ambient or slightly elevated temperatures at high impulsive strain rates. In both cases slip by dislocation movement is restricted.

A steeper gradient of the shock front causes an increased fracture stress for spalling (8) and there is a decreased amount of ductility (or increased cleavage) in spalls with a rough surface.(24). The increased fracture stress maybe due to an increase in hardness caused by a steeper wave front, cleavage increases because there is insufficient time for plastic strain

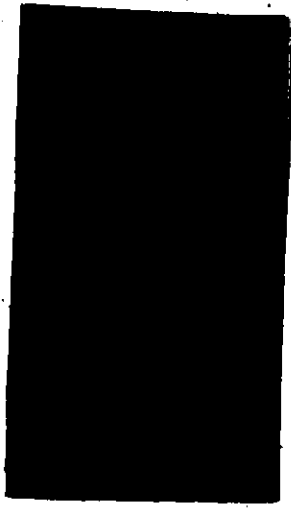
to blunt the crack tip (27,28). Cleavage in a pendulum type impact test is more frequent than that in the slow fracture of the same steel. It seems therefore not surprising that the cleavage mode is the predominant fracture mode for spalling in α iron. The stress gradient of the shock wave can be related to the critical stress that causes spalling as follows: (28)

$$\sigma_c = A + B \left(\frac{d\sigma}{dx} \right)^{1/2} \quad (11.)$$

in which A and B are constant and $d\sigma/dx$ is the stress gradient. This is graphically shown in fig. 26 for copper and for aluminium (26). We have no such data for iron.

A different criterion for the critical fracture stress is that using the total impulse (I) of the stress wave. This theory implies that a lower stress applied during a longer time will cause spalling as would a higher stress during a shorter period of time. For loading in the micro-second range the time dependent (impulse) criterion and the stress gradient criterion both give satisfactory results (28).

Fig. 25 (a) Cleavage crack arrested by a pre-existing twin. (b) Cleavage crack passing through deformation twins.



b

Fig 26 Characteristic spall curves for aluminium and copper.



(B) SMOOTH FACED SPALLS

Much of what was said above only applies to spalling caused by the single stress wave that we find when the phase transition has not complicated the shape of the stress profile. The fig. 23b gives a schematic representation of the shape of the pressure wave showing the plastic I and the Plastic II wave fronts and the rarefaction trail caused by the transformation of α iron to ϵ iron. It shows in four

different steps how a sharp fronted tension wave is created when the plastic II wave interacts with the rarefaction trail. This sharp tension front is formed in a very thin layer of material at a certain distance from the surface (distance A in fig. 23b). This sharp tensile front creates a spall with a smooth machined like surface (8,24). In addition to a single smooth faced spall several rough faced spalls may form after the smooth fracture has formed. TEM fractographs show that the structure of the smooth fracture face consists of very fine dimples (24). Below the fracture face there are microvoids, most of which are spherical in shape. We note that spherical cavities are also formed in explosively loaded iron at 300°C (10) these cavities are not connected by cracks. See Fig. 27. The fracture is transgranular with little regard for the microstructure of the steel. The origin of the dimples could not be established as they were too small. It is estimated that there are approximately 100 dimples per grain. The fracture has to be classified as a ductile decohesion although the ductility is only apparent at a very small scale. No cleavage surfaces are present despite the fact that some of the grains would have been suitably oriented for cleavage to take place. The explanation for this ductile decohesion by the coalescence of

microvoids involves the following factors:

- 1) The stress front is extremely small and steep.
- 2) The material maybe undergoing a phase change involving volume charges.
- 3) Liquids subjected to an impulsive wave may "cavitate".

Cavitation is the formation of small bubbles (microvoids) in an area where the cohesive strength of the liquid is exceeded. A similar thing appears to be taking place here.

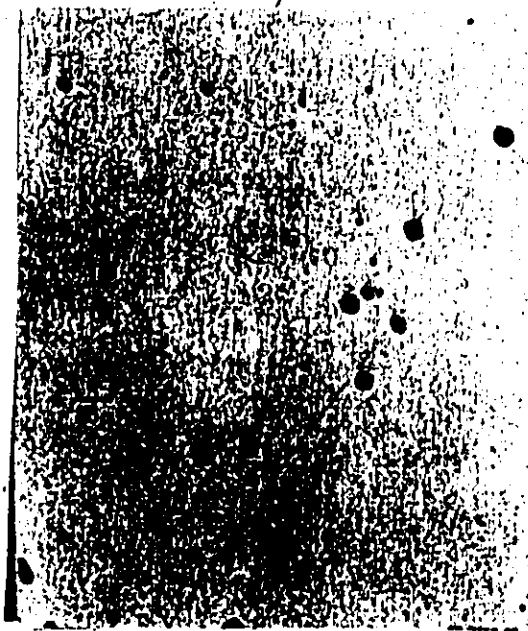


Fig. 27 . Damage in Armco iron at 300°C. Impact velocity = 505 ft/sec; Target thickness = 0.250 in; Projectile thickness = 0.093 in.

The processes of the atomic movements in a shock front are presently not well understood (two possible models were given in fig. 22). Present observation, techniques and time measurements methods do not allow direct measurements of the pressure gradient and of the atomic movements therein. The orders of magnitude of the phenomena involved are as follows: the atoms in a metal lattice vibrate with a period of 10^{-8} micro seconds; an impulsive wave lasts in the order of 10 micro seconds and the time of the pressure rise is in the order of 10^{-1} micro seconds. A shock front of 0.1 mm width represents a layer of 10^5 atoms thick. For the formation of smooth spalls a stress of 13 GPa (2×10^6 psi) is necessary. The theoretical strength of iron, based on atom decohesion and surface tension considerations, is approximately equal to one tenth of the modulus of elasticity of 200 GPa (3×10^7 psi). The strength observed in iron whiskers is 13 GPa (2×10^6 psi). The stresses that may be found in an impulsive shock wave front are thus not far from the theoretical strength of iron.

The three or four fold increase of the fracture stress (for spalling) under the impulsive loading versus that of the fracture of steel under slow loading is related to the following factors:

1) The fracture nucleates in many points and each fracture propagates only for approximately one grain diameter in the case of the rough spalls and less in the case of smooth spalls. I am of the opinion that in such cases the nucleation of all these cracks is probably the stage that requires more energy than the propagation of these cracks. The threshold energy for the formation of a continuous spall is therefore large compared to that in conventional fracturing of low carbon steel. The brittle fracture at conventional strain rates generally involves the propagation of a single crack. In this case it is the crack propagation stress that is the critical parameter and not the stresses for the nucleation of the crack. The conventional ductile fracture of low carbon steel involves the nucleation and the coalescence of microvoids. The number of microvoids that cause the fracture is small compared to that found in a smooth spall. Furthermore in the first instance dislocation movements assist in the nucleation of the microcracks, which is not the case in the second instance.

2) The triaxial nature of the stresses in impulsive loading raises the stress level at which fracture occurs (16,17).

3) A spall forms in material that has been work hardened by the initial plastic compression wave or

waves. This partially explains (for rough faced spalls) that the critical fracture stress for spalling is larger for higher impulsive waves. (27)

6.2.1.3 Surface Energy - The surface energy of a material influences its ability to resist fracture. The Griffith theory for brittle cracks states that the critical stress for crack propagation increases with the square root of a "pseudo" surface energy and with the square root of the reciprocal of the crack length from which it starts propagating. The crack will propagate when the strain energy released by crack propagation is larger than the kinetic energy of the crack propagation plus that of the surface energy (or a "pseudo" surface energy) needed to form new crack surface. The kinetic energy is related to the displacement of metal during the formation of the crack. In fact the strain energy created by the impulsive wave converts to kinetic and to surface energy in the case of crack propagation. The kinetic energy increases with the crack velocity. It has been suggested that the kinetic energy of the movement of the crack is related to the terminal velocity of a brittle crack, which has been calculated to be 0.37 times the dilatational wave velocity for steel. It is the initial nucleation of the micro cracks in the ferrite matrix that requires the largest stresses

because the crack size of the Griffith equation is smallest. (We note that at the ultimate crack length of one atomic spacing we obtain the theoretical strength of a material or roughly 0.1 times the modulus of elasticity). The stress near the tip of a moving crack (σ) at a time (t) is related to the crack velocity (V) as follows: (27)

$$\sigma = E \cdot t \left[\frac{A \cdot \sigma_0 \cdot V}{S} - \dot{\epsilon}_p \right] \quad (12.)$$

in which E is the modulus of elasticity, A is a constant σ_0 is the applied stress, S is the specific surface energy and $\dot{\epsilon}_p$ is the local plastic strain rate. This formula cannot be solved by itself as the local plastic strain rate $\dot{\epsilon}_p$ depends on the stress at the crack tip σ .

6.2.2 Corner fractures, fracture cones and center-line fractures.

It is only in regions where the wave front is parallel to the surface that it causes spalling. In the corners of the body the reflected waves from two intersecting surfaces can add to produce high tensile stresses which may cause corner fractures. A limiting case is when the intersecting surfaces meet at infinity: A "center fracture" may form in the center between such parallel surfaces. It has been found (6) that fractures form according to the rules of wave reflection. These rules are shown schematically in Fig. 28: The tensile

stresses F_1 and F_2 combine to form a corner fracture starting in corner P, stresses F_2 and F_3 form a fracture near the center of the trapezoid that runs into the corner Q and the stresses F_1 and F_3 interact to form a center fracture at O approximately half way between the opposing free surfaces that reflected F_1 and F_3 . The three fractures meet in one point in the center of this trapezoid shape. A center line fracture is shown in figure 29.

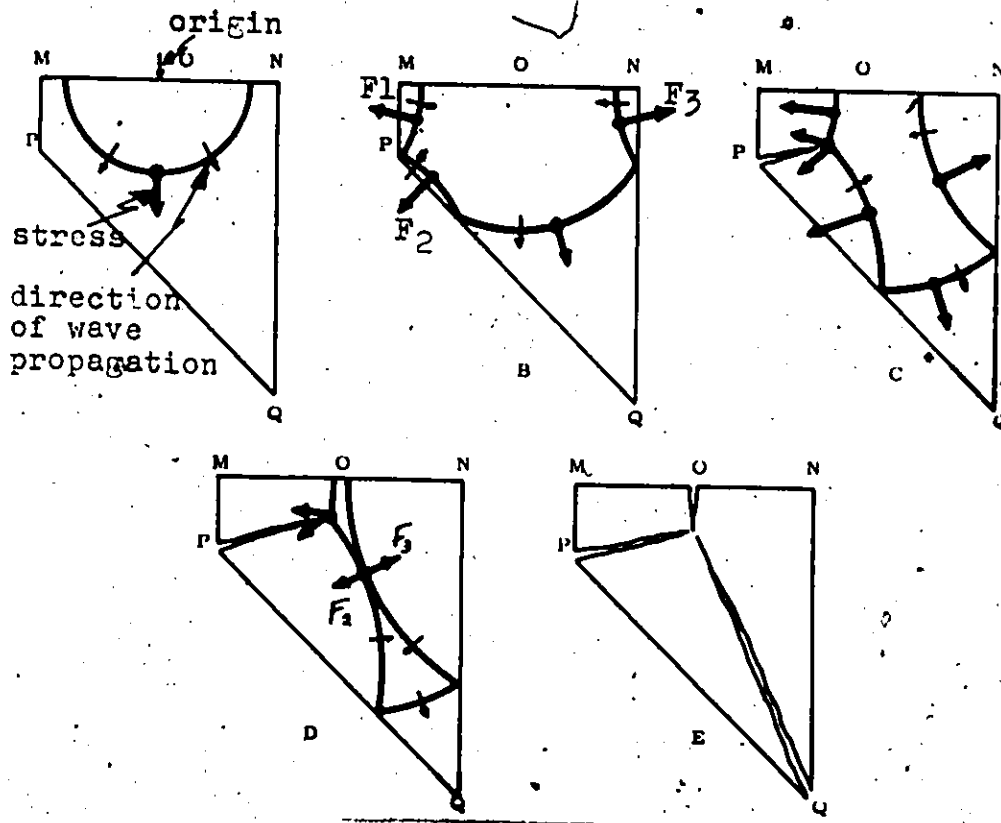


Fig. 28 Schematic representation of corner and center-line fractures.



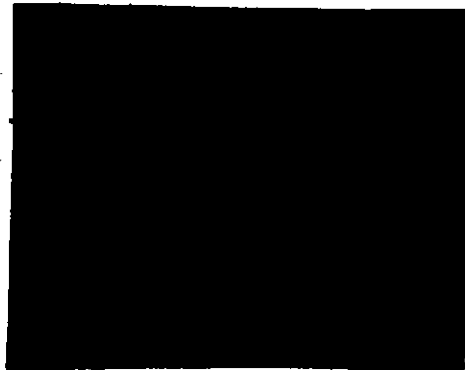
Figure 29- Cross section of mild steel plate loaded by two opposing contact charges. Notice craters and centerline fracture.

The shear waves that form as a result of oblique reflections of the compressive wave travel at approximately half the speed of the tensile wave. They play no role in the crack formation in this case. It is only when the material is severely compressed and the formation of tensile cracks is suppressed (the Bridgeman effect - (16) that shear fractures are found. This shall be treated in the discussion of the stress condition of impulsively loaded hollow cylinders. A cone shaped fracture is found in a cylinder at the end opposite to that at which the explosive was detonated. It forms when the corner fractures meet in the centre of the cylinder. (Fig. 30) The angle between the face of the cone fracture and the bottom face of the cylinder can be used to determine the velocity of the wave propagation (C) if the detonation

velocity (D) of the explosive is known:

$$C = D \cos \alpha \quad (13)$$

Fig. 30 Brass cylinder
with fracture cone.



An interesting type of corner fracture is shown in fig. 31 (29). A polyethylene sleeve with a diameter of 1.17-m (3 ft 10 in), a length of 3.7 m (12 ft 7 in) and a wall thickness of 4 cm (1.625 in) under went an accidental fall from a height of 20 m (65 ft). This corresponds with an impact velocity of approximately 18 m/s (60 ft/s). The sleeve fell straight down in an axial direction on a concrete floor. The compression wave so created traveled from the bottom to the top end of the cylinder which contained a V - shaped groove. The interaction of the tension waves reflected at both sides of the V caused a completely brittle crack of a length of 1.5 m (5 ft). This is interesting as polyethylene will elongate by 400% when it is subjected to a slow strain rate. We note that the purpose of the sleeve was to limit damages from possible explosions inside

the sleeve. The V-shaped grooves in these sleeves were changed to U-shaped grooves to give the sleeves added impact resistance. Another interesting fracture is that found is a plate loaded on its edge (1). The plate will split along the center plane parallel to the surfaces as a result of tensile waves reflected from both surfaces.



Fig. 31 Corner fracture of polyethylene sleeve by pressure wave traveling from down to up.

A different type of fracture caused by stress waves is the "second fracture" in a brittle material that forms from the elastic pressure wave liberated from an adjacent "first" fracture. The sudden formation of a crack in a statically stressed material relieves the stress and a compressive wave travels into the material away from the crack surface. The reflection and the interference of this reflected wave with existing stresses, possibly the shear wave released from the same fracture, may cause a second fracture. I found an example of this type of fracture in a 4 m (12 ft) long steel bar with a cross sectional area 5 x 5 cm (2 x 2 in) (31). The bar failed with two brittle failures near the two ends of the bar under a tensile stress of 0.44 GPa (65,000 psi). The material had a charpy-V notch impact energy of 2.7 at - 18°C (2 ft 1b 0°F). The failure happened at an ambient temperature of 0°F. Similar fractures were observed in explosively loaded polymers. (5).

Interesting results were obtained (32,33) by studying the nature of stress waves created from fractures by measuring with strain gauges the acoustic emissions during brittle fracturing. The discussion of this work lies outside the scope of this report.

6.2.3 Tensile fractures caused by divergent compressive waves (radial fractures)

Considering the situation that a hollow cylinder is loaded by an explosion within the cylinder and that it is strong enough not to fracture as a result of the internal pressure. The material adjacent to the explosive is severely compressed. Material further away from the explosive does not yet experience the effects of the explosion until the pressure wave arrives at approximately 4 micro seconds per linear inch of distance later. This material will thus serve to restrain the expansion of the metal that is adjacent to the explosive. The result is that no fractures form in this phase provided that lateral flow of the material is not possible (Fig. 32). However as the pressure wave moves outward, tensile cracks form in a radial direction. The tensile stress arises from the enlargement of an annular layer as it moves outward. The tangential particle velocity in this ring (ds/dt) is given by:

$$\frac{ds}{dt} = \theta \cdot \frac{dr}{dt}$$

14.

whereby θ is the angle over which the tangential particle velocity is measured and dr/dt is the radial particle velocity. From the above formula with θ equal to the angle between adjacent fractures, ds/dt is found to equal the critical impact velocity (V_c).

The angle θ is then given by the ratio v_r/v where v is the radial particle velocity. The formula for the number of cracks (N) or for the number of pieces (N) that will form in the cylinder is then:

$$N = \frac{2\pi v}{v_c}$$

This theory has not yet been proven to give quantitatively correct results although there seems to be some agreement for medium or heavy walled cylinders.

Another example of fracture due to diverging waves is what maybe found in a solid rod that was coated with an explosive. Fig. 33 shows the nine pieces that originated from a 2.5 cm diameter solid steel rod coated with a thick layer of explosive. The fracture faces are roughly radial. They have a rough and fibrous surface texture that is very different from conventional fractures in steel. The original converging compressive wave will have an increasing peak pressure the closer the wave front gets to the center of the rod. In the center of the rod the pressure may rise to two or more orders of magnitude above the yield stress of the metal. In some cases the high pressure may force the metal to extrude out of the center of the rod. After the pressure wave passes the center of the rod it continues as a diverging pressure wave, creating radial cracks as described.

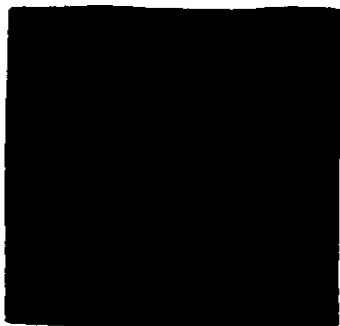


Fig. 32 internally loaded cylinder.

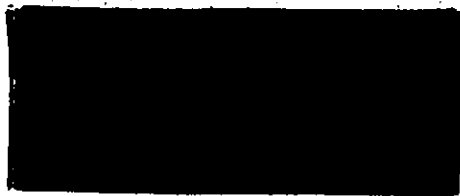


Fig. 33 mild steel rod fractured by coating of explosive.

6.2.4 Tensile fractures caused in the pressure relief phase.

This category contains the tensile fractures that are not caused by the initial dilatational waves. They may be brittle tensile fractures that run at a high velocity away from the source of the explosion. One may compare these cracks to the final running cracks in a breaking plate of glass. The dilatational wave created at detonation runs approximately 3.25 times faster than a crack in iron has been observed to propagate (1,33). This wave may leave behind a large number of small fractures but it passes before the cracks have time to propagate. The pressure of the expanding gasses in the pressure relief phase may exert a high mechanical force that may tend to open up such cracks. It may supply the driving energy for crack propagation. It is the same force that propels the various pieces of fractured metal-other than spalls-away from the origin of the explosion after their formation by the initial dilatational or shear waves.

I examined several such fractures in a steel drilling pipe which suffered an accidental explosion (14). The pipe has at its bottom end a thread at the exterior side with which it was coupled to a lower section of the drilling pipe. A contamination with explosive at the thread caused an explosion which traveled upward into the pipe. The explosion fractured a 32 cm long non-threaded section of the pipe starting from the thread. The pipe is made of a tempered martensitic steel that is case hardened at the exterior face. The exterior diameter of the pipe is 37.5 mm (1.5 in) and the wall thickness is 12.5 mm (0.5 in). The 32 cm long section examined had fractured into two semi-cylinders by diametrical fractures. Each of these semi-cylinders broke into two parts. I examined three of the so obtained four parts.

The longest piece has one diametrical fracture that is essentially flat, the other has a wavy edge at the outer surface, but is straight at the inner surface. In combination with this wavy edge are bifurcation cracks. One of the two other pieces also has bifurcation cracks at the exterior surface. The maximum depth of the bifurcation cracks is 2.5 mm. All bifurcation cracks run away from the threaded end of the pipe. The longest bifurcation crack found was

43 mm. long. This crack was nearest to the threaded end. The shortest bifurcation crack was 1 mm long and it was furthest away from the threaded end.

Fig. 34 shows the relationship between the length of a bifurcation crack and its distance from the threaded end. The relationship seems to be parabolic. This would mean that the bifurcation crack length depends on the energy available for the propagation of the main crack.

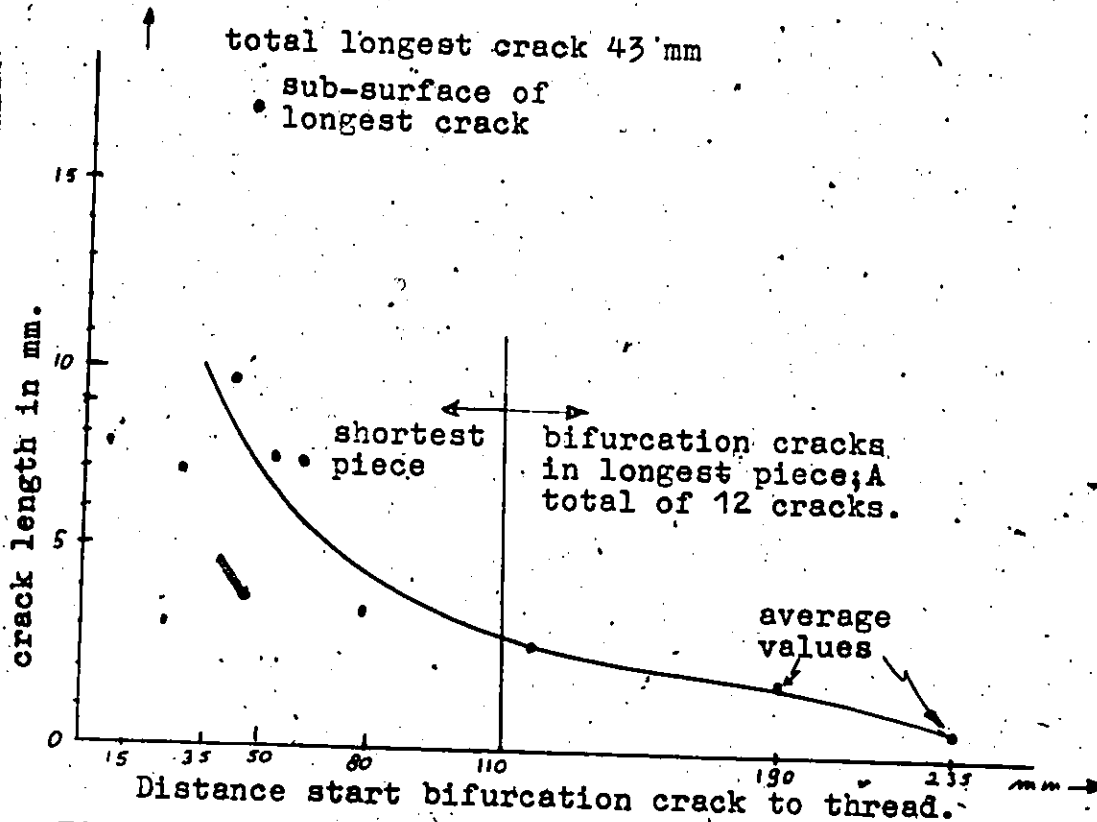


Fig. 34 Length of bifurcation cracks vs. distance to thread.

The direction of the bifurcation cracks proves that the fracture propagated upward from the thread of the drilling pipe. A chevron pattern is visible on the diametrical fracture at the exterior and at the interior pipe surfaces - fig. 35. Normally chevron markings are parallel to the direction of the movement of the crack front. Chevron marks have the appearance of a bird's feather with the root of the feather at the fracture origin. This is the way that the chevron marks run at the diametrical fracture that shows the wavy edge although the marks are somewhat irregular at the wavy edge itself. The other diametrical fracture in the same piece shows marking that run upward and inward at the interior edge as would the markings of a feather laid down on the fracture with the root of the feather at the pipe thread. However, at the straight exterior edge they run as with the root of the feather away from the pipe thread. What was said above is shown in a photograph of the two opposing diametrical fractures in fig. 35. The side with the wavy edge is at the right and the fracture propagated from the bottom to the top of fig. 35. The inverse chevron marks at the straight edge fracture face maybe explained by assuming that the crack front was more advanced at the hardened case than in the interior of the wall of the pipe. This does not

explain why if this surface crack ran so fast, it is this edge that is straight while the opposite exterior edge with normal chevron marks is wavy. There are other theories that explain inverse chevron marks but they do not apply here or they do not explain the phenomena observed.

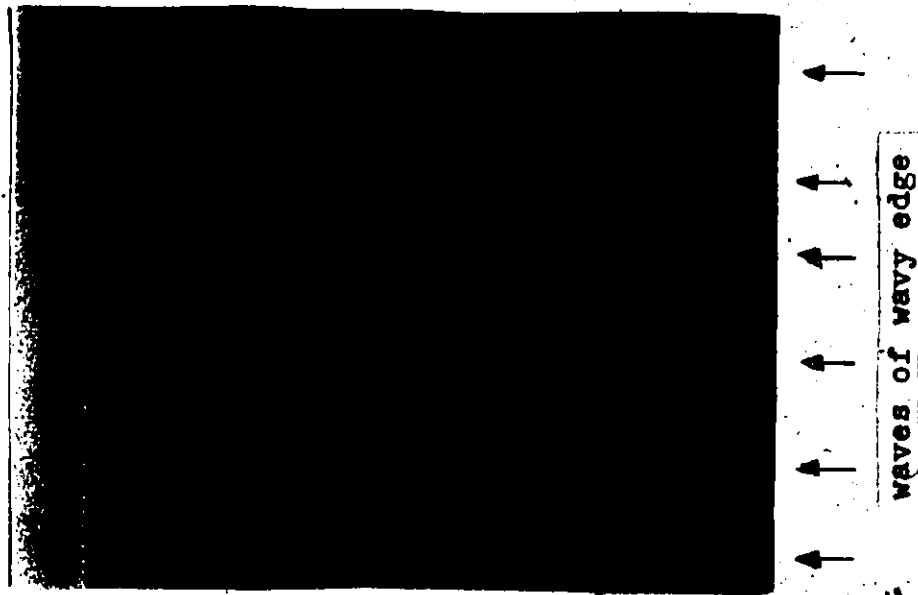


Fig. 35 Diametral tensile fractures in explosively fractured drilling pipe. The fracture traveled from down to up. The wavy edge is at the right, the inverse chevron marks are at the extreme left. 2x.

There were a total of 17 waves or undulations in the plane of the diametrical fracture of the largest of the pieces examined (14). The average wave length was 9 mm (0.35 in). At the start of twelve of these waves there are small bifurcation cracks that separate from the main fracture face. It appears thus that bifurcation of the fracture is related to

the wavy path of the fracture edge or vice versa. This is not always the case. Fig. 31 shows the undulating path of the brittle fracture in polyethylene. I found another example of a wavy fracture path in the accidental explosion of a 100 gallon propane tank (34). The tank failed due to an excessive pressure through a circumferential fracture. The fracture was a pure shear fracture. In the final 50% to 70% of the fracture surface a waviness with a wavelength of 25 to 38 mm (1 to 1.5 in) was observed. There was no sign of any bifurcation cracking in this case as bifurcation cracking seems to be limited to fractures in the tensile mode. Bifurcation of cracks has been linked (for fractures in glass) with cracks traveling at some maximum crack velocity. This speed would be half of the shear wave velocity (5). For steel the maximum crack velocity is reported to be approximately 1,800 m/s (6,000 ft/s) or 57% of the shear wave velocity. (1). Assuming that the maximum crack velocity has been reached it is easy to conceive that when more stress is available at the crack tip than is required to propagate the single crack that a second crack could form. Whichever of these two cracks gets ahead causes a drop in the stress available at the other crack tip; the crack that is ahead will continue while the other crack will stop. The

anisotropy in the grain structure of the pipe will favor the propagation of longitudinal cracks over radial cracks.

The three semi-cylindrical pieces of drilling pipe examined have common fracture surfaces. The longest and the shortest pieces have bifurcation cracks while the piece of medium length has none: The longest piece has twelve cracks where it borders the piece of medium length while the shortest piece has three cracks where it borders the longest piece fig. 36a and three cracks where it borders the medium length piece - fig. 36b. (The short piece was slightly less than semi-cylindrical where it borders the other piece). The impression given by the location of the bifurcation cracks is that the shortest piece was lifted of the other two pieces and that then the longest piece lifted of the medium length piece. Two of the more or less radial fractures that form the top end of the shortest and the longest pieces grew from bifurcation cracks. This is indicated by chevron marks and by the original angle with which they leave the diametrical plane. The radial fracture at the top end of the longest piece is arrested by the straight edged diametrical fracture.

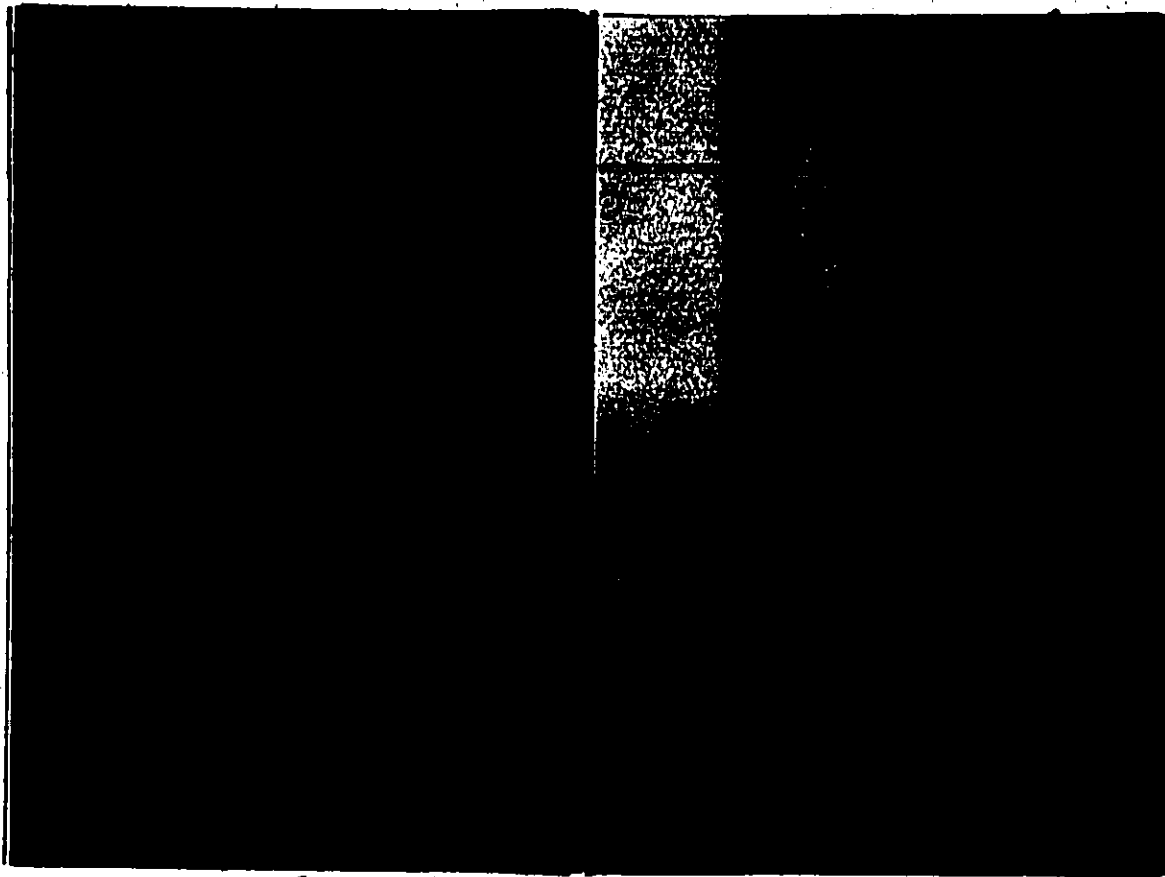


Fig. 36 a and b The bifurcation cracks in the shortest length pipe section - see text.

6.3 Shear fractures

Shear fractures are common in explosively loaded metals. The fractures take place along trajectories of maximum shear stresses. Fig. 37 shows the maximum shear trajectories for an internally loaded hollow cylinder and for a surface load on a flat surface. Figure 38 shows an example of the fractures in an externally loaded aluminum hollow cylinder. Comparing figures 32 and 38, it appears that star like fractures are formed at the interior

surface of the hollow cylinder in the case of external as well as internal loading. Shear fractures follow the same direction as the Luders bands in steel which is a phenomenon of yield along trajectories of maximum shear. At the explosively loaded drilling pipe thread there are axial shear fractures that meet the interior surface of the pipe at a 45° angle (14). The sheared area is slightly curved with the concave side facing inward. (See fig. 39).

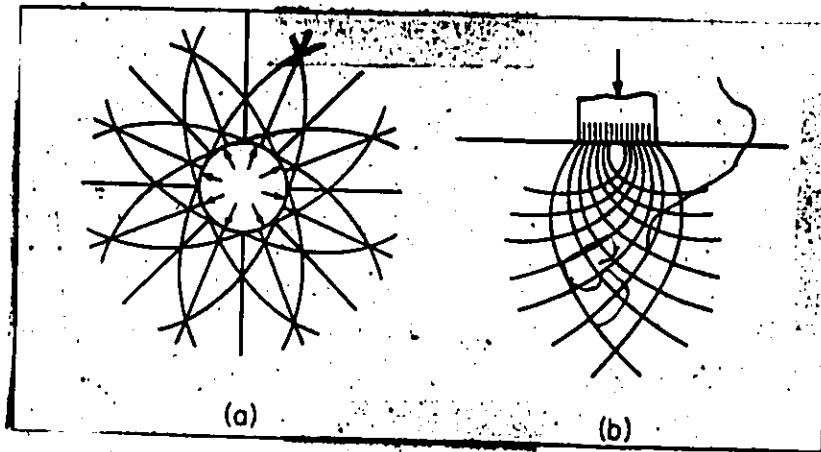


Fig. 37 a and b Fields of maximum shear trajectories for (a) Circular Hole under internal pressure, and (b) Flat surface under contact pressure.

Fig. 38 Cross section of 248T aluminum alloy hollow cylinder loaded with layer of explosive on outer surface



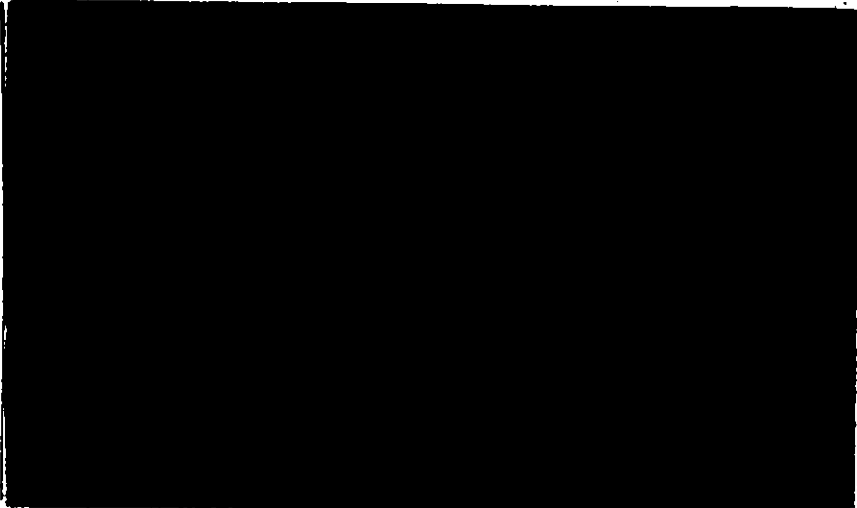


Fig. 39 a and b. A piece of the drilling pipe thread showing tensile and shear fractures (mag. 1.3x)

The sheared area had a smooth and shiny appearance, which is usual in shear. The deformations on the shear plane show that the fracture surfaces were forced over one another with great force. The structure being brittle martensite (Photograph fig. 40), this means that large forces and or large ambient pressures were present.

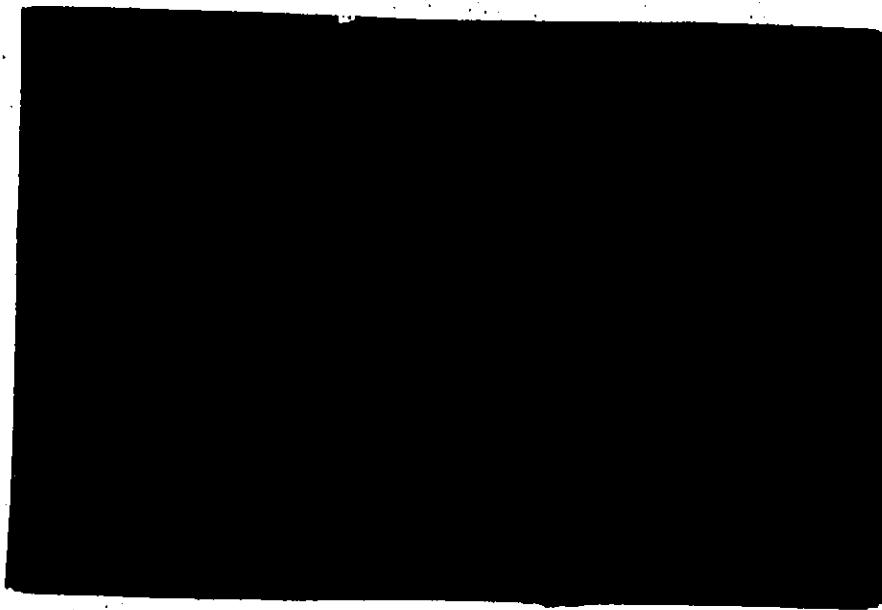


Fig. 40. The structure of the drilling pipe.

At the threads of the pipe up to 55% of the pipe thickness broke as a shear fracture while the remaining 45% of the wall thickness broke as a tensile fracture. (see fig. 39). In these tensile fractures, we found chevron marks that indicate that these fractures started at the exterior surface and that they ran inward to meet the shear fractures. We found fourteen separate tensile fracture origins that were exposed while there were at least another six suspected fracture origins hidden in closed cracks. (see section 6.2.3). At the start of the non-threaded straight section there is a shear lip that covers approximately 20% of the wall thickness. Further away from the thread the shear lip virtually disappears.

(It is visible as a line in fig. 35). The area of the largest shear lips shows some plastic deformation at the interior surface with a local increase in the radius of curvature of the pipe from 6.35 to 11.4 mm (0.25 to 0.45 in).

Pressure has the following effects on the fracture of steel (15,16): .

- 1) It suppresses the growth and the coalescence of microvoids in ferrite,
- 2) It retards the cleavage fracture of pearlite,
- 3) Cementite becomes somewhat ductile and it may fracture in shear and,
- 4) The planar shear mode of fracture dominates over cup and cone, cleavage or intergranular type fractures.

6.4 The cutting of metal with explosives

Explosives placed in contact with or near to a metal object can shear the object depending on the size of the charge and the strength of the object.

This cutting action of an explosive can be enhanced by three factors:

- 1) A V-shaped cavity left in the face of the explosive that is in contact with the metal. This is shown in fig. 41. The V-shape creates a relatively narrow column of explosion products in the center of the V.
- 2) The V-shaped cavity in the explosive can be placed at

a certain distance from the object to be cut. This stand-off distance is usually measured in the order of several inches.

- 3) The V-shaped cavity can be lined with a metal of the same shape. This creates high velocity jet of metal particles (fig. 42) that collides with the metal surface. The pressure (say 27 GPa or 4×10^6 psi) and the high temperatures (say 800°C) created in this impact forces the target material to flow or shear out of the path of this jet. Holes or cuts of a depth of 6 inches in mild steel can so be obtained. (Fig. 43)

Fig. 41 - Cratering effect produced by conically shaped charge.



Fig. 42 Diagram showing the mode of deformation and break up of a conical liner. (After Kolsky, Snow and Shearman)





Fig. 43 - Cross section of steel target showing jet penetration from a cylindrical shaped charge

The cutting action is caused by the jet of metal particles that moves at a velocity in the order of 1,800 to 2,400 m/s (6,000 to 8,000 ft/s). This means that the dilatational pressure wave created by the detonation and by the impact with the metal jet is always ahead of the jet itself. The hardening effect of the initial dilatational wave does not seem to influence the depth of penetration of the jet to a great extent (18).

The surface of a hole created in a low carbon steel target with a medium carbon steel lined charge has a martensitic structure: Some of the target material reached the A_c1 temperature of 727°C . Fig. 18 gives the hardness profile measured from the cavity into the parent metal of the target. The hardness profile thus obtained (18) compares with the one obtained with an ordinary surface charge (fig. 19). Shaped charges are applied for their cutting action in metal working, armor piercing

weapons such as bazookas or anti-tank rockets, the tapping of blast furnaces, the piercing of an oil-well casing, in salvaging operations, and in mining operations.

7. DISLOCATIONS AND SHOCK WAVES.

The Rayleigh wave velocity or the transverse sound wave velocity are generally the limiting velocities for dislocations as at these levels the energy of the dislocations becomes infinite. (20,35,36) At high speeds the dislocations are slowed down by this relativistic effect, by dislocation damping and by dynamic effects. High speed edge dislocations are an effective source of vacancies as conservative motions of such dislocations would require supersonic velocities. (36) It has been calculated, in ref. 36, that edge dislocations of the same sign will attract each other when they move at or near to the transverse wave velocity. This phenomenon would assist the formation of micro-cracks when edge dislocations join together and thus increase the Burgers vector. Screw dislocations would behave normally at high velocities. From these data it would seem that the dilatational stress waves that cause fracture travel about twice as fast as conventional dislocations.

Figure 22 shows one model for the behavior of the lattice in a wave front that uses dislocations as a "bridge" between two, otherwise regular metal lattices of the compressed and of the uncompressed metal. In order for such dislocations to remain in the moving shock front they have to move at super-sonic speeds.

Super-sonic speeds have been proposed by Eshelby - see ref. 20-for the edge dislocation. Figure 44 shows the proposed model when a complete series of atoms at one side of the slip plane is in perfect misfit. This would be the same type of condition that is found in a metal such as iron at the moment when a diffusionless phase transformation takes place.

The dislocation behavior in impulsive shock waves and at pressure levels whereby metals may react like liquids is presently in the hypothesis stage.

Fig. 44 Eshelby's
supersonic dislocation



8. CONCLUSIONS

The detonation of an explosive in the near vicinity of a metal creates a shock wave with a maximum pressure in the order of 3.5 GPa to 40 GPa (0.5 to 5.8 million psi) in the metal. The length of the impulsive wave is in the order of 4 cm and it lasts several micro seconds. The passing stress wave causes work hardening without any substantial amount of physical deformation having been done. There is presently a lack of data on the mechanism that causes the hardening. Little is known to date about the dislocation and vacancy behavior in shock loaded materials. The velocity of the pressure wave is about twice the velocity at which move conventional dislocations and about three and a half times the velocity at which brittle cracks have been observed to propagate in steel. The maximum crack velocity in a material is related to the speed at which the stress field at the tip of the crack can rearrange itself and it is related to the speed at which lattice defects move.

In certain conditions of loading, it is the initial compressive wave that causes fracturing. This is the case when a diverging wave causes tangential stresses that create radial fractures. This is found in the internal loading of hollow cylinders. Also the initial pressure maybe sufficient to cause shear fractures in thin walled specimens.

The most common fracture phenomena in impulsively loaded metals are caused when the initial compressive wave is reflected against a free surface with a change of sign. The tensile wave so created may cause the spalling phenomenon or when two reflected waves reinforce each other, corner or centerline fractures can occur.

The fact that iron undergoes a phase transformation from the bcc to the hcp lattice at a pressure of 13 GPa (approximately 2 million psi) causes the pressure wave to break up in two principal fronts that travel at different speeds. This phenomenon, apart from complicating other effects of the pressure wave, may result in the formation of a spall with a smooth surface while otherwise spalls have rough surfaces. Smooth faced spalls are formed by a ductile decohesion process whereby approximately 100 micro voids form per grain. The coalescence of these voids - which lie in a very thin layer of material - causes the spall. Rough faced spalls form by the cleavage of individual grains and by the final shear between adjacent cleavage facets.

In the fracture of a steel drilling pipe that was caused by an accidental explosion the failure of the area closest to the source of the explosion took place by shear fractures near the interior and by tensile fractures near the exterior of the pipe. This combination of

fracture modes is common in the loading of hollow cylinders. The fast running cracks that created several pieces of metal some distance away from the source of the explosion show an interesting bifurcation phenomenon that seems to be related to the stress available for the crack propagation. The bifurcation cracks also seem to be influenced by the way the various parts of the pipe separated from one another. There is an interesting case of "inverse" chevron marks on a fracture face of a piece away from the source of the explosion.

Many of the mechanisms found in impulsive loading such as the formation of deformation twins and the formation of brittle cracks seem to be similar to those found in the low temperature deformation of steel. In both cases the relative mobility of dislocations is limited.

In the field of impulsive loading explosives themselves and stress wave behavior below the level of the phase transformation are reasonably well covered. Most of the knowledge in impulsive loading of materials has started to take serious form only in the last twenty five years. Many new and sophisticated observation techniques are recently becoming available. There is hope that these techniques as well as an increased interest in this field will fill in a large gap in presently available data.

LITERATURE LIST

1. J.S. Rinehart, J. Pearson, Behavior of metals under impulsive loads, ASM 1965.
2. J.S. Rinehart, J. Pearson, Explosive working of metals, Pergamon press. N.Y. 1963.
3. G.L. Ludolph, Lehrbuch der mechanica, J.B. Wolters, Netherlands 1959
4. G. Dieter, Mechanical metallurgy, Mc Graw Hill, 1961.
5. H. Kolsky, D. Rader, Fracture 1, ed. Liebowitz. Academic press, N.Y. 1968
6. J.S. Rinehart, On fractures caused by explosions and impacts, Quarterly Colorado School of Mines V 55, 4, 1960
7. A.S. Appleton, The metallurgical effects of shock waves, Appl. Mat. Res. Oct. 1965
8. I.C. Skidmore, An introduction to shock waves in solids, Appl. Mat. Res. July 1965
9. D.N. Pipkorn et al, MÜsbauer effect in iron under very high pressure, Phys. Rev. V 135- 6A, 1964
- 10 D.R. Curran, Dynamic mechanical behavior of iron, Trans. AM. Inst. Min. (metall.) Engrs. V 215 1959, p. 151
- 11 D. Bancroft et al, Polymorphism of iron at high pressures, J. Appl. Phys. V 27- 3 1956
- 12 E.G. Zukas et al, Iron and steel under impulsive loading, Resp. of met. to high velocity deformation, AIME conf. 9, p. 343
- 13 J.S. Rinehart, J. Appl. Phys. V 22- 9, 1951
- 14 E. Vos, Analysis of a steel pipe failure as a result of an accidental explosion, May 1975, un. publ.
- 15 T.E. Davidson, G.S. Ansel, Trans. AIME (met.) V 245, 1969, p 2389
- 16 P.W. Briġeman, Studies in large plastic flow and fracture, Mc Graw Hill, N.Y. 1952
- 17 H.P. Tardif et al, Response of metals to high velocity deformation, AIME Conf 9, 1960, p. 389
- 18 S. Singh et al, L. Appl. Phys. V 27- 6 1956, p. 617
- 19 C.S. Smith, Response of metals to high velocity deformation, AIME Conf. 9 1960, p. 309

- 20 E. Weertman, Response of metals to high velocity deformation, AIME Conf. 9, 1960, p. 205
- 21 G.E. Dieter, Response of metals to high velocity deformation, AIME Conf. 1960, p. 410
- 22 C.S. Smith, Trans. AIME (met), 1958
- 23 J.S. Rinehart, Scabbing of metals, multiple scabbing, J. Appl. Phys. V 23- 11 1952
- 24 E.E. Banks, Spall fractures in low carbon steel, J. Iron & Steel Inst. 1968, p. 1022
- 25 T.C. Lindley, Acta Met. 1967- 1
- 26 L.E. Keachele et al, Acta Met. 1969, p.463
- 27 F.A. McClintock; A.S. Argon, Mechanical behavior of materials, Addison-Wesley(Canada) Ltd. 1966
- 28 J.C. Peck et al, Critical stress versus stress gradient theory of spall fractures, Int. J. Fract. Mech. V 5, 1969 297
- 29 E. Vos, Unpublished work, E. Vos Reg'd file 249
- 30 J.J. Gillman et al, Dynamic fracture by spallation in metals, Int. J. Fract. Mech. v 6- 2 1970
- 31 E. Vos, Unpublished work, E. Vos reg'd file 78
- 32 H. Kolsky, Engineering fracture mechanics, 1973, V 5, p. 513
- 33 H.C. van Elst, The intermittent propagation of brittle fracture in steel, Trans AIME (met), V 230, Apr. 1964, p 760
- 34 E. Vos, Unpublished work, E. Vos Reg'd file 228
- 35 C.H. Ma, Dislocation damping in a shock stress field, Acta Met. V. 22, 1974, p. 675
- 36 J.M. Kelley et al, Dislocation dynamics and precursor attenuation, J. Appl. Phys, V. 18 1967, p. 4044
- 37 E.R. Parker, Brittle behavior of engineering structures, J. Willey & Sons Inc. N.Y. 1957
- 38 W.A. Allen, Surface motion induced by shock waves in steel, J. Appl. Phys. V. 24- 9. 1953
- 39 J.S. Buchanan et al, Measurements of high intensity stress pulses, Br. J. of Appl. Phys. V. 10, 1959, p. 293

- 40 W.E. Drummond, Multiple shock production, J. Appl. Phys. V. 28- 9 1957, p. 998
- 41 L.W. O'Brien, Response of metals to high velocity deformation, 1960, p. 371
- 42 C.M. Fowler, Response of metals to high velocity deformation, 1960, p. 275
- 43 J. Milkowitz, Elastic waves created during tensile fracture, J. Appl. Mech. 1953, p. 122